International Journal of Physical Research, 1 3(1) (2025) 12-22

International Journal of Physical Research

Website: www.sciencepubco.com/index.php/IJPR
https://doi.org/10.14419/h3rchs22
Research paper

P, Q, and R branches of the pure oxygen A-band at 762 nm

Muhammad Ahmad AL-Jalali *

A former Prof. Dr. at the Department of Physics, Faculty of Science, Taif University, Kingdom of Saudi Arabia
**Corresponding author E-mail: aljalaliphys@gmail.com*

Received: May 4, 2025, Accepted: May 25, 2025, Published: May 29, 2025

Abstract

Oxygen A-band absorption spectra exhibit interference between O2 monomer (with a discrete line at 762 nm) and O2 dimol (which also exhibits a band spectrum at 762 nm) absorption. Analysis of the absorbance spectrum between 750 nm and 770 nm reveals P, Q, and R branches, characteristic of rovibrational transitions. Pure oxygen spectra were analyzed at pressures ranging from 1 to 25 bar and at temperatures of 298 K, 323 K, 348 K, and 373 K using advanced data analysis methods. Integrated absorbance, Gaussian and Lorentzian full width at half maximum height (FWHM), and maximum absorbance peak positions were calculated for the R and P branches, and relevant formulas were deduced.

Keywords: *O2 Monomer; O2 Dimol; Absorbance; FWHM; Gaussian Width; Lorentzian Width; Branches; Rovibrational.*

1. Introduction

The oxygen A-band spectrum at 762 nm is vital for atmospheric studies and remote sensing. It features a strong molecular oxygen absorption line, enabling scientists to measure key atmospheric properties, including temperature, pressure, and humidity. By analyzing the absorption characteristics of this spectral band, researchers can accurately detect oxygen concentrations and quantify atmospheric gases. This capability is essential for understanding atmospheric composition, climate dynamics, and weather forecasting. Additionally, the oxygen A-band is crucial for satellite-based remote sensing platforms, assisting in calibrating and validating atmospheric models, radiative transfer calculations, and monitoring changes in Earth's atmosphere over time. Thus, it is an invaluable tool for environmental research and climate science [1-10].

The oxygen A-band, centered around 762 nm, is known as the A-oxygen absorption band in atmospheric physics and as the atmospheric oxygen band in meteorology. The oxygen molecule (O_2) is characterized by a zero electric dipole moment and a paramagnetic triplet ground state (${}^3O_2[X\,{}^3\Sigma_g^-(0), m_s = 0, \pm 1]$) [11-14]. A molecular infrared spectrum requires an electrical dipole moment; theoretically, oxygen's vibrational and rotational energy states cannot be directly excited by radiation. However, experimental evidence shows that oxygen gas possesses both discrete and continuous absorption spectra. The absorption or emission spectrum of an oxygen molecule occurs in two steps: first, a collision induces an electric dipole moment (μ) to deviate from its zero value ($\partial\mu / \partial q \neq 0$). Second, incident radiation is absorbed, exciting the molecule to a higher energy level. This excitation process is termed collision-induced absorption (CIA). [15-17]. the experimental sample containing both O_2 dimol (O_2-O_2) and O_2 monomers (O-O). The O_2 monomer exhibits a discrete absorption line with P, Q, and R rotational branches. The second-lowest diamagnetic singlet electronic excitation energy from the O_2 ground state is [18-21]:

$$ {}^3O_2[X\,{}^3\Sigma_g^-(\upsilon=0)] + 762\ nm \rightarrow {}^1O_2[b\,{}^1\Sigma_g^+(\upsilon=0)] \quad (1) $$

A continuous absorption band is characteristic of O_2 dimol, resulting from collision-induced absorption (CIA) involving two O_2 molecules in electrically excited states. The second-lowest electronic excitation energies originate from the ground state of the O_2 dimol through the following processes:

$$ {}^3\Sigma_g^-(\upsilon=0)\ {}^3\Sigma_g^-(\upsilon=0) + 762\ nm \rightarrow {}^3\Sigma_g^-(\upsilon=0)\ {}^1\Sigma_g^+(\upsilon=0) \quad (2) $$

Both forms of oxygen have absorption bands centered at 762 nm. As pressure increases, a phenomenon known as line-mixing occurs within the branches, leading to overlap between the lines in the absorption band. This overlap makes it challenging to distinguish between the two forms, particularly in contexts where collision-induced spectroscopy is commonly used. [22-26].

The objective of this paper is to present a mathematical enhancement technique that conceptualizes each spectral branch as an envelope encompassing all overlapping absorption lines. This methodology employs the Voigt deconvolution technique alongside the Savitzky-

Golay method to refine the analytical process. In addition, integrated absorption, maximum absorbance, full width at half-maximum height, Gaussian width, and Lorentzian width are calculated, and some mathematical formulae and semi-empirical equations are deduced.

2. Theoretical background

Unperturbed solution results of the total energy equation according to the Born–Oppenheimer approximation solution of the diatomic Schrödinger equation were given as a total energy [27],[28]. The observed fine structure in infrared bands indicates that the molecule can be treated as a vibrating rotator (rigid rotor), with its rovibrational energy characterized by vibrational and rotational quantum numbers v, J:

$$E_{v,J} = E_{rot} + E_{vib} = BJ(J+1) + \left(v + \frac{1}{2}\right)\hbar\omega_e \;, v, J = 0,\ 1,\ 2,\ 3\ \ldots \text{etc.}$$
$$\omega_e = \sqrt{\frac{k}{\mu}}, \quad \mu = reduced\ mass, k = \text{force constant}, B = \frac{\hbar^2}{2\mu R^2} = \text{rotational constant}, \tag{3}$$

The band gap between energy levels tends to decrease rapidly for higher values of frequency until it reaches the dissociation energy (D). The vibrational transition is called the fundamental band; other bands for transitions from the ground vibrational state to 2, 3, 4, etc., levels are called overtones, where infrared spectroscopy may prevail. The rotational energy levels when J=0,1,2,3… have energy 0,2B,6B,12B, etc. Transitions between levels obey the selection rule. Then $\Delta J = \pm 1$ The simple rigid rotor consists of a series of equidistant absorption lines with frequencies 2B,4B,6B… etc., where microwave spectroscopy and far infrared may prevail in these situations. For real molecular gas, anharmonic vibration energy and rotation energy for the non-rigid rotor are given as rovibrational energies (in terms of wave numbers) by expanding as a McLaurin series expansion [29], [30]:

$$\frac{E_{v,J}}{hc}(cm)^{-1} = \underbrace{\omega_e\left(v + ½\right) - \omega_e x_e\left(v + ½\right)^2}_{G(v)} + \ldots + \underbrace{B_v J(J+1) - D_v J^2(J+1)^2}_{F(v,J)} + \ldots$$
$$T(v,J) = G(v) + F(v,J), \quad B_v = B_e - \alpha_e\left(v + \frac{1}{2}\right) \tag{4}$$

The coefficients $\omega_e, \omega_e x_e, B_v, D_v \ldots$ etc. They are called the harmonic and anharmonic rovibrational parameters. B_e rotational constant at the minimum of the potential curve and the vibration-dependent rotation constant B_v (the rotational constant associated with a vibrational state v). α_e is a constant depending upon the shape of the potential. For a given initial vibrational transition v and final state v', also with the quantum number of the initial rotational state being *J* and that of the final rotational state being *J',* considering only transitions that involve the ground vibration state, the wave number change is (D_v is neglected):

$$\bar{\upsilon} = T(v',J') - T(v,J) = G(v') - G(v) + F(v',J') - F(v,J)$$
$$D_v \approx B_v \Rightarrow \tag{5}$$
$$\bar{\upsilon} = T(v',J') - T(v,J) = \bar{\upsilon}_0 + B_v' J'(J'+1) - B_v J(J+1)$$

From the relation above, the infrared spectrum is a vibration-rotation spectrum. When $J' = J + 1$, there is a net absorption of rotational energy; when $J' = J - 1$, there is a net emission of rotational energy (although overall there is absorption of energy). The usual selection rules are: $\Delta J = 0, \pm 1$, $\Delta v = \pm 1$
If $\Delta J = +1$ we obtained the R branch ("rich", the molecule gains rotational energy), If $\Delta J = -1$ we obtained, the P branch ("poor", the molecule loses rotational energy), If $\Delta J = 0$ we obtained Q branch, this branch could appear in IR spectrum of polyatomic molecule and the molecule must have a permanent electric dipole moment. Neglecting the centrifugal distortion terms, this gives [31], [32]:

$$\bar{\upsilon}_R(\Delta J = +1) = \bar{\upsilon}_0 + 2B_v' + (3B_v' - B_v)J + (B_v' - B_v)J^2 \quad J = 0,1,2,3,\ldots R\ branch$$
$$\bar{\upsilon}_P(\Delta J = -1) = \bar{\upsilon}_0 - (B_v' + B_v)J + (B_v' - B_v)J^2 \quad J = 1,2,3,\ldots P\ branch \tag{6}$$
$$\bar{\upsilon}_Q(\Delta J = 0) = \bar{\upsilon}_0 \qquad Q\ branch$$

Instead of the previous equations, one could find the exact equation for branches, which is like the equation of a parabola; they can be fitted to the same parabolic equation:

$$\bar{\upsilon} = \bar{\upsilon}_0 + (B_v' + B_v)m + (B_v' - B_v)m^2$$
$$m = J + 1 = 1,2,3,\ldots, R(0), R(1), \ldots lines$$
$$m = -J = -1,-2,-3,\ldots, P(1), p(2), \ldots lines \tag{7}$$
$$m = 0 \ \ for\ zero\ gap\ at\ \bar{\upsilon}_0$$

The infrared spectrum consists of a series of transitions due to the different rotational states involved. The Spectral Calculator (www.spectralcalc.com) to the spectra of oxygen gas as is shown in figure (1) indicates that it is filled with the spectral rotational lines in the region between 750 -770 nm. where the intensity of the Q branch is zero (null gap) at the band origin $\bar{\upsilon}_0$ =762 nm but intensities of P, R branches increase with increasing J on either side of it, reaches a maximum and then slowly decrease.it seems R branch is stronger than P branch.

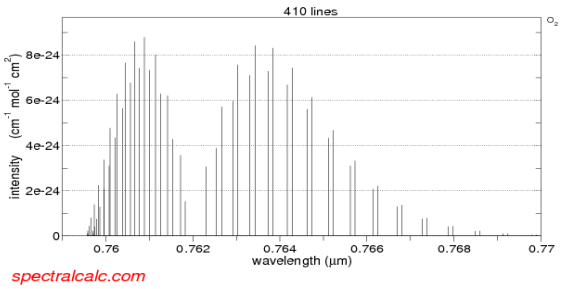

Fig. 1: Typical Spectrum Intensity of Oxygen A Band Spectrum with P, Q, and R Branches at Room Temperature as A Function of Wavelength in the Range of 0.75 to 0.77 Micrometers.

At high pressures, the rotational structure of a band is not resolved, then P and R branches appear as envelopes (wings) extending on either side of the band origin, $\bar{\upsilon}_0$ =762 nm. The P and R can be recognized in these envelopes, and deconvolution methods can measure their separation. From the peaks (maximum absorbance) of envelopes, the rotational constant B can be computed roughly if temperature is known, and the value of J at which maxima occur (maximum population) is given by:

$$J_{\max} = \sqrt{\frac{kT}{2Bhc}} - \frac{1}{2} = \sqrt{\frac{T}{2\theta_{rot}}} - \frac{1}{2} \approx \frac{1}{2}\left(\sqrt{T} - 1\right)$$
$$\theta_{rot} = \frac{hc}{k} B = 1.44B\ K \tag{8}$$

Where θ_{rot} is the rotational characteristic temperature (for oxygen = 2.1 K), by ignoring rovibrational interaction, the wave numbers of R and P branch lines at the maximum of the envelopes and the distance between these maxima (peaks), which corresponds to the $J_{max,}$ are given by:

$$if\ \ B'_v = B_v = B \Rightarrow$$
$$\bar{\upsilon}_R^{\max}(\Delta J = +1) = \bar{\upsilon}_0 + 2B + 2B\left[\sqrt{\frac{kT}{2Bhc}} - \frac{1}{2}\right]$$
$$\bar{\upsilon}_P^{\max}(\Delta J = -1) = \bar{\upsilon}_0 - 2B\left[\sqrt{\frac{kT}{2Bhc}} - \frac{1}{2}\right] \tag{9}$$
$$\bar{\upsilon}_R^{\max} - \bar{\upsilon}_P^{\max} = \sqrt{\frac{8BkT}{hc}} \approx \sqrt{5.5BT}$$

Experimentally, the wave numbers of the lines of the O2 band are given from experimental results, and then the differences and second differences of successive lines are calculated. As Deslandres first noticed [33], the separation of successive lines increases nearly linearly since the second difference is a constant within the measurement accuracy. From this, it follows that the lines can be represented by a formula of the type (Fortrat parabola):

$$\bar{\upsilon} = c + dm + em^2$$
$$m = 0, \pm 1, \pm 2, \ldots etc \tag{10}$$

Where c, d, and e are constants, and m is a whole number that represents the successive lines. If we allow m to take on negative values as well as positive ones, we can choose c, d, and e in such a way that we begin the numbering (m = 0) at any desired line. However, it appears that there is one point in the series where a line is missing. Later, we will see that it is convenient to designate this missing line as the m = zero line or the null line, that is, $c = \bar{\upsilon}_0$. This specific place in the band is commonly called the zero gap or null-line gap (Q branch). The coefficient d of m in the formula is obtained from the mean value of the observed first differences between successive spectral lines, $\Delta\bar{\upsilon}$=d. The coefficient e of m^2 in the formula is obtained from the mean value of the observed second differences between successive values of the first difference values of the experimental spectral line, $\Delta^2\bar{\upsilon}$=2e. Of course, one has to be careful when choosing the wave number of both these lines, which includes some error of observation. The R and P branches, corresponding to positive and negative *m* values, respectively, together form a single series of lines described by the same formula. Equation (10), representing a parabola, was first used by Fortrat, and this parabola is thus called the Fortrat parabola, a term used throughout this paper [29], [33]. Comparing theoretical and experimental procedures, one can find semi-empirical expressions:

$$\bar{\upsilon} = \bar{\upsilon}_0 + (B'_v + B_v)m + (B'_v - B_v)m^2 = c + dm + em^2$$
$$B'_v + B_v = d = \frac{1}{2}\Delta\bar{\upsilon}, B'_v - B_v = e = \frac{1}{2}\Delta^2\bar{\upsilon} \tag{11}$$
$$if\ \ e = 0 \Rightarrow d = 2B_v \Rightarrow \bar{\upsilon} = \bar{\upsilon}_0 + 2B_v m = c + dm$$

An alternative method of determining the rotational constant is by the use of the separation $\Delta\bar{\upsilon}$(m) of the successive lines and the increase of this separation, the second difference $\Delta^2\bar{\upsilon}$(m), according to equation (7):

$$\Delta\bar{\upsilon}(m) = \bar{\upsilon}(m+1) - \bar{\upsilon}(m) = 2B'_v + 2(B'_v - B_v)m$$
$$\Delta^2\bar{\upsilon}(m) = \Delta\bar{\upsilon}(m+1) - \Delta\bar{\upsilon}(m) = 2(B'_v - B_v) \tag{12}$$

From these two semi-empirical equations, one could find rotational constants.

3. Experimental results

Experimental measurements were chosen to measure the absorbance spectrum as a function of wavelength in the near-infrared region, specifically ranging from 750 to 770 nm. These measurements were taken under pressures varying from 1 bar to 25 bar and at temperatures of 298 K, 323 K, 348 K, and 373 K. Figures 2 and 3 illustrate the raw samples alongside the pure oxygen absorbance spectrum as a function of wavelength. Experimental procedures were described in our recent papers on pure oxygen gas [34-37]. Figure 2 shows that absorbance in the rotational-vibrational band is minimal at the band origin (672 nm), then increases with J on both sides, reaching a maximum before gradually decreasing. R branches exhibit more substantial absorbance than P branches. At constant pressure, absorbance in both branches decreases with increasing temperature, while at constant temperature, it increases with increasing pressure, where increased collision-induced absorption (CIA) reduces resolution. The rotational structure is unresolved, with P and R branches appearing as wings flanking the band origin. The maxima of these branches are discernible, and their separation can be mathematically determined.

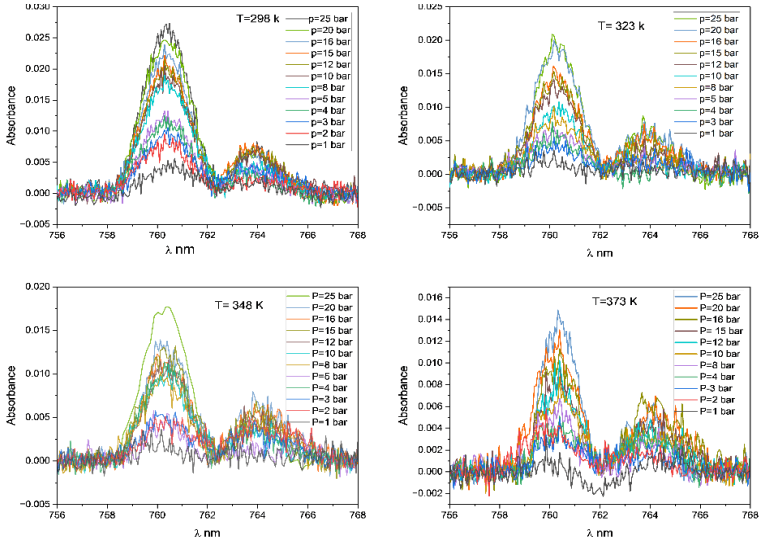

Fig. 2: Experimental Absorption Spectra of the O_2 A Band at Various Pressures and Different Temperatures as A Function of Wavelength.

Figure 3 shows the decrease in absorption intensity of oxygen gas with increasing temperature for 16 samples randomly selected from the 48 samples studied in this research at many different temperatures. This behavior can be attributed to several factors related to the increase in the kinetic energy of the gas molecules as temperature rises, where the population of molecules in the lower energy states becomes less significant compared to those in higher energy states because more molecules can occupy these higher energy states. Consequently, fewer molecules are available to absorb photons at certain wavelengths, leading to a decrease in the overall absorption intensity as the temperature rises.

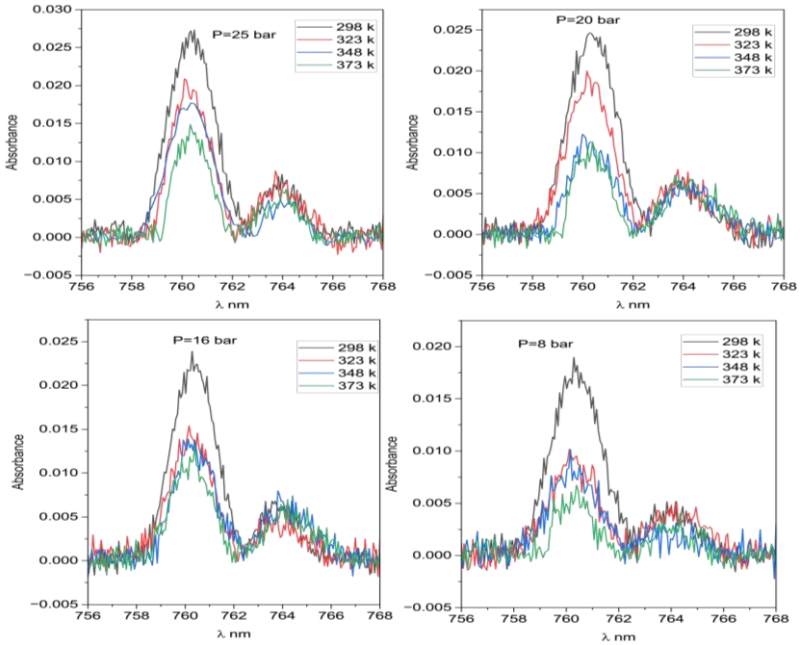

Fig. 3: Some Samples (Sixteen Representative Samples from the 48 Analyzed) Are Taken from Figure 1 to Illustrate How Temperature Increases Affect Absorbance; Specifically, Absorbance Decreases as Temperature Rises.

4. Data analysis

Origin Pro Lab software was used for data analysis to separate the P and R branches from each other. The absolute area under each branch(A), central wavelength ($\bar{\upsilon}_0$ =762), Gaussian (Γ_G), Lorentzian (Γ_L) width, full width at half-maximum height (FWHM), and maximum absorbance in each branch were exactly defined through the deconvolution method of the Voigt profile function (for mathematical equations see [38-41]), and the Savitzky-Golay method was used for some quick and easy calculations. Forty-eight samples were subjected to data analysis under pressures extended from 1 to 25 bar at 298 K, 323 K, 348 K, and 373 K.
Figure 4 illustrates a comprehensive data analysis of the total oxygen spectrum between 750 and 772 nm at various temperatures, distinguishing the P and R branches from each other by using the Voigt deconvolution method [36]. The Q branches consistently appear at 762 nm (as mentioned above, the intensity of the Q branch is zero (null gap) at the band origin $\bar{\upsilon}_0$ =762 nm). At constant temperatures, all figures in Figure 4 indicate that the peaks for each branch show an increase in maximum value, absorbance, and integrated intensity as pressure increases. Additionally, these findings are consistent with the data and results presented in Figure 2.

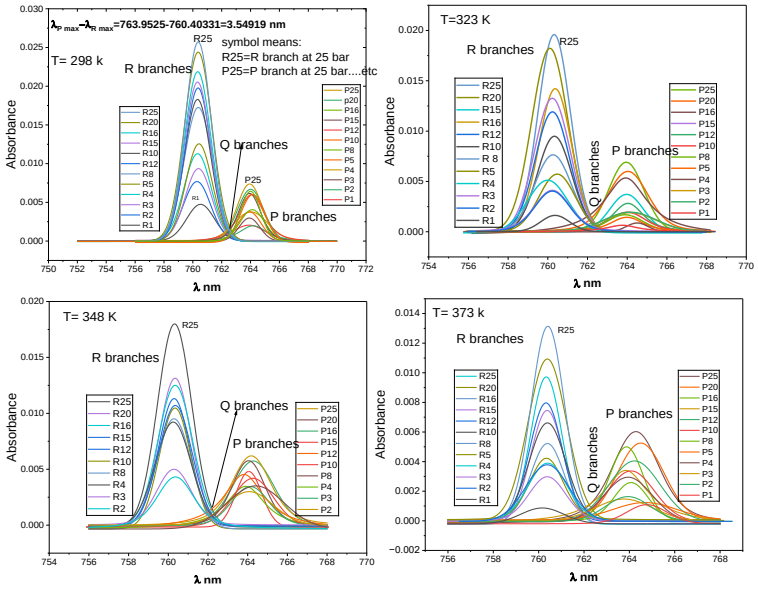

Fig. 4: Voigt Deconvolution Method of Experimental Spectral Lines to Separate P and R Branches from Each Other.

The rotational structure of the band, with well-defined R and P branches at nearly 360.3 nm and 363.6 nm, respectively, is evident throughout the studied pressure range. The wavelengths of the rotational lines and branch peaks remain constant within the 0.2 nm experimental error, and pressure-induced line broadening is negligible compared to this error.

5. Results and discussion

In both P and R branches, the absorption intensity and maximum absorbance increase with pressure at constant temperature, while they primarily decrease with temperature at constant pressure. Also, the conflict between Gaussian and Lorentzian widths as a function of pressures and temperatures directly affects absorption intensity.
However, the work [13], [22], [42], [43] studied collision-induced absorption changes in the 762 nm A band at pressures from 20 bar to 200 bar and showed that collision-induced absorption (CIA) changes are proportional to the square of oxygen pressure. However, in the field of pressures studied in this work, the contribution of collision-induced absorption due to O_2–O_2 molecules (O_2 dimol) did not exceed 0.010 of the total absorption intensity at a pressure of 25 bar. For this reason, the contribution of collision-induced absorption to the absorption intensity in the field of pressures below 20 bar is very weak, so the pure absorption intensity of free oxygen molecules will prevail. The Lorentzian contribution of the increase in the width of the rotational lines, caused by the increase in pressure, did not exceed the amount of error caused by the baseline shift of the spectrometer when spectra were recorded, due to the increase in the presumption of refraction of the gas when its pressure increased, which is consistent with what is stated in the work [44].
These results can be studied and clarified by dividing them into the following paragraphs:

5.1. Effect of pressures and temperatures on the absorbance of branches

Figure 5 shows a linear relationship between the integrated absorbance of P and R branches as a function of pressures at temperatures 298 K, 323 K,348 K, and 373 K.

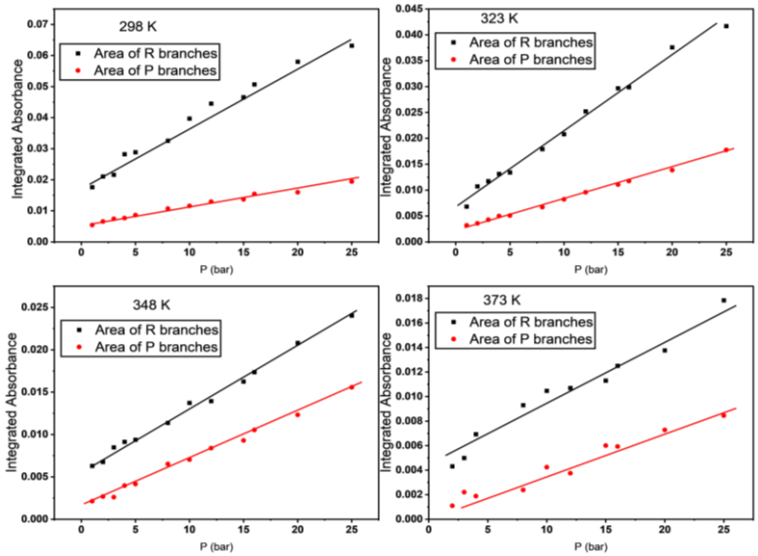

Fig. 5: Dependency of Integrated Absorption on Pressure for P and R Branches, with Separate Figures for Each Temperature.

Figure 6 also separates the results of R branches from the P branches, where both have a linear relationship with a positive slope with pressures, but a poor absorbance was observed at 373 K and vice versa.

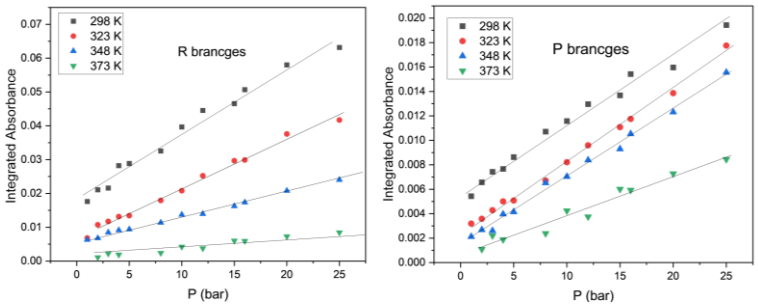

Fig. 6: Pressure Dependence of the Integrated Absorption of the P and R Branches, Each Branch Considered Separately, at Different Constant Temperatures.

Figure 7 shows clearly that the absorption intensities in the R and P branches decrease with temperature at constant pressures due to changes in the population of vibrational states, effects of broadening, and collisional interactions among molecules. Each of these factors contributes to lowering the effective absorption as temperatures rise.

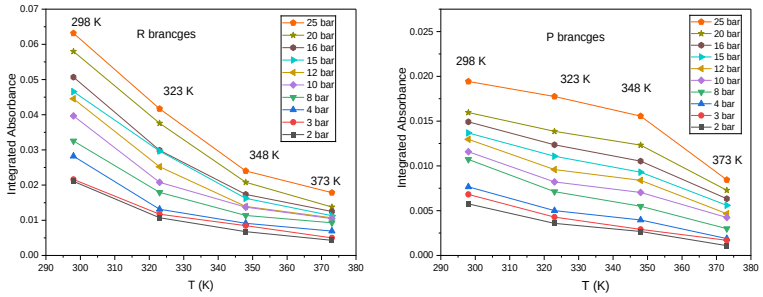

Fig. 7: Temperature Dependence of the Integrated Absorption of the P and R Branches, Each Branch Analyzed Separately, Under Various Constant Pressures.

Figure 8 shows a linear relationship between the maximum absorbance of the P and R branches as a function of pressure, at the peak of the envelopes, which decreases as temperatures rise. At a temperature of 298 K, the data appears to exhibit two stages of linearity. The first stage, from 1 bar to 8 bar, is characterized by a sharp slope, while the second stage, from 8 bar to 25 bar, features a slower slope and greater stability. Of course, maximum absorption at P branches is less than at R branches and noisier.

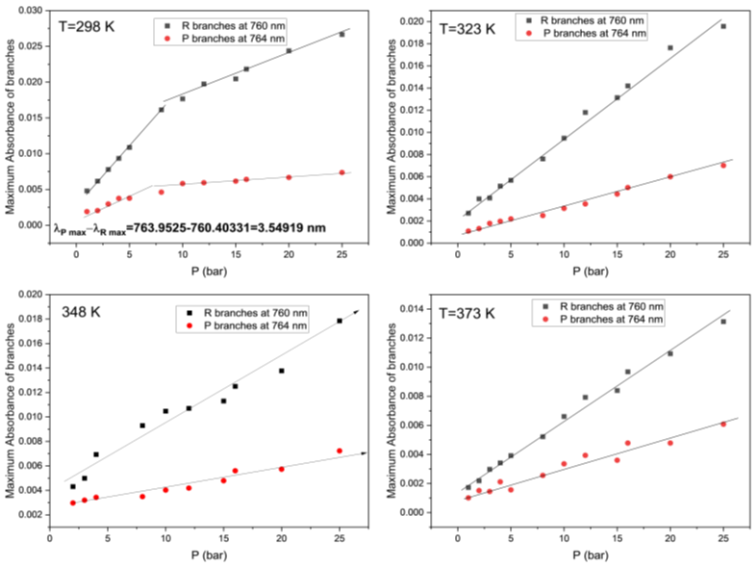

Fig. 8: Maximum Absorption of the P and R Branches, Each Figure at A Separate Temperature, As A Function of Pressure.

Figure 9 displays the maximum absorption intensity of the P and R branches separately versus pressure at specific temperatures, illustrating that absorption is inversely proportional to temperature and directly proportional to pressure in both branches.

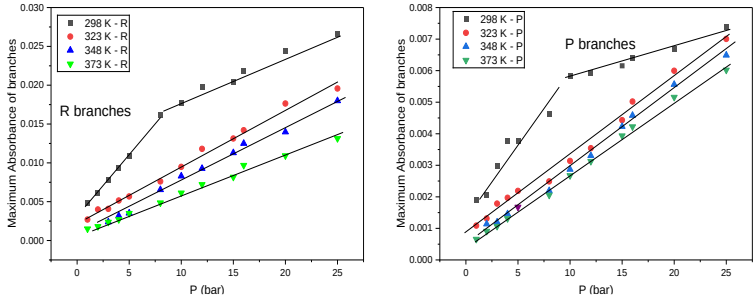

Fig. 9: Maximum Absorption of The P and R Branches, Each Branch Separately, as A Function of Pressure Under Varying Temperatures.

In summary, the decrease in absorption intensity of the R and P branches of the oxygen spectrum with increasing temperature is mainly due to changes in the population of vibrational states, effects of broadening, and collisional interactions among molecules. Each of these factors contributes to lowering the effective absorption as temperatures rise.

5.2. Simple comparison between the Voigt deconvolution and Savitzky-Golay methods

The Voigt method is explained in detail and is essential for the research. In contrast, the Savitzky-Golay method is a simpler and faster approach that smooths the spectral line to enhance the visibility of the branches. This method allows for the calculation of maximum absorbance and the areas of the spectral lines for each branch. For more complex studies, such as those involving Doppler broadening and pressure broadening, the Voigt method is specifically suited for handling intricate analyses.
Figures 10A and 11A illustrate the Savitzky-Golay method used to differentiate between the P and R branches compared with the Voigt deconvolution method. Additionally, it presents the absorbance of both branches as a function of wavelength., Figure 10B and 11B illustrates the analysis of the maximum absorbance points of the envelopes corresponding to the P and R branches as a function of pressure; the results are nearly the same only for maximum absorbance and integrated absorbance, but the Voigt method is still more reliable and accurate especially in calculating other rotational constants.

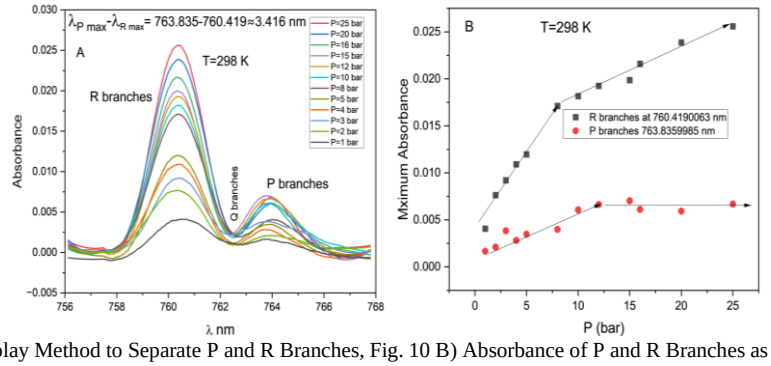

Fig. 10: A) Savitzky-Golay Method to Separate P and R Branches, Fig. 10 B) Absorbance of P and R Branches as A Function of Pressures.

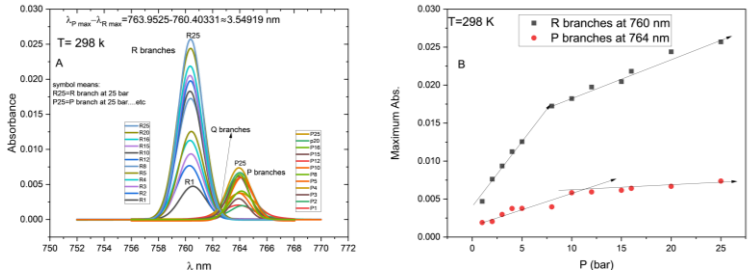

Fig. 11: A) Voigt Decomposition Method to Separate P and R Branches, Fig. 11 B) Absorbance of P and R Branches as A Function of Pressure for Comparison between the Two Methods.

Experimentally, P-R branch peak separation $\left(\bar{\upsilon}_R^{\max}-\bar{\upsilon}_P^{\max}\right)_{\exp.}=45-68\,cm^{-1}$ From semi-empirical expressions (9), the values of $\left(\bar{\upsilon}_R^{\max}-\bar{\upsilon}_P^{\max}\right)_{calc.}$ could be calculated as follows:

$$\begin{aligned}
&\bar{\upsilon}_R^{\max}-\bar{\upsilon}_P^{\max}=\sqrt{\frac{8BkT}{hc}}\\
&\left(\bar{\upsilon}_R^{\max}-\bar{\upsilon}_P^{\max}\right)_{298K}=48.479\,cm^{-1}\\
&\left(\bar{\upsilon}_R^{\max}-\bar{\upsilon}_P^{\max}\right)_{323K}=50.754\,cm^{-1}\\
&\left(\bar{\upsilon}_R^{\max}-\bar{\upsilon}_P^{\max}\right)_{323K}=52.682\,cm^{-1}\\
&\left(\bar{\upsilon}_R^{\max}-\bar{\upsilon}_P^{\max}\right)_{373K}=54.541\,cm^{-1}
\end{aligned} \tag{13}$$

5.3. Gaussian and Lorentzian widths in P and R branches

Doppler (Gaussian) broadening was gradually decreasing with increasing pressure, while pressure (Lorentzian) broadening was mostly negligible below 12 bar. It became slightly noticeable above 16 bars, but it did not impact Doppler broadening. This suggests that collision-induced absorption is minimal within this pressure range. In other words, the interplay between thermal and collisional effects is weak. Additionally, Lorentzian broadening can be disregarded at low pressures. The experimental observation that absorption intensities in the R and P branches decrease with increasing temperature is linked to higher rates of collisions and pressure effects. These factors can cause the redistribution of molecular populations away from the states that contribute to the specific transitions in those branches. Figures 12 and 13 indicate that the situation in this sample is unstable. It's important to note that the slopes of the straight lines in both figures represent the Doppler broadening coefficients for both the P and R branches. This is because the contribution of pressure broadening is not significant at this range of pressures, which means initially, the initial effect of collision-induced absorption (CIA) was not observed in this pressure range [for the term pressure broadening see 45].

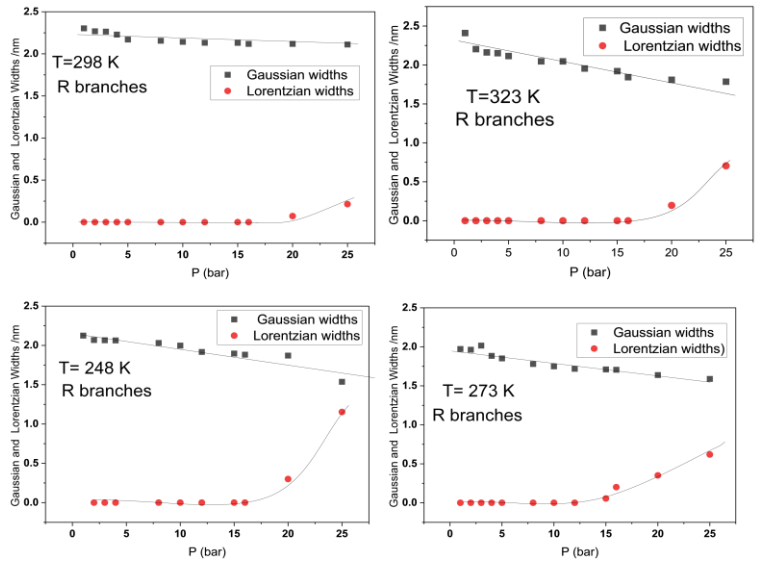

Fig. 12: Gaussian and Lorentzian Widths in R Branches as A Function of Pressure at Different Temperatures.

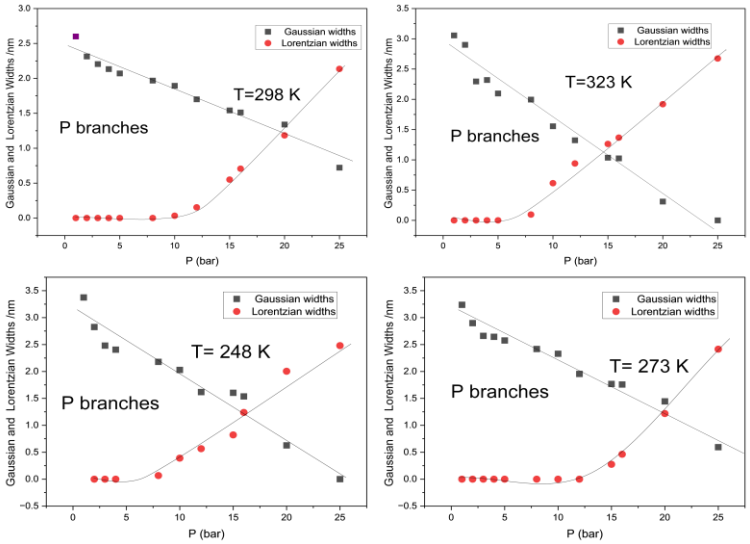

Fig. 13: Gaussian and Lorentzian Widths in P Branches as A Function of Pressure at Different Temperatures.

It is clear from the graphs that the competition between Gaussian width and Lorentzian width appears clearly above 15 bar pressures.

5.4. Fortrat parabola method

As indicated in the previous paragraph, and through equations 9,10,11, and 12, one of the spectral lines was chosen from among 48 spectral lines, and the peaks were calculated using the Origin Lab program, and the steps mentioned in the previous paragraph were applied. The graph was drawn, and then the rotational constants were calculated and compared with what was calculated manually. Figure (14) shows the quadratic relationship between the peak values of the spectral line as a function of the positive and negative m values, where m equals zero, corresponding to the wavelength of 762 nm (Q branch), which was chosen according to the Fortrat method. The method was applied to more than five samples, and the results were similar; therefore, using a single spectral line was sufficient. The participation of O_2 dimol was weak and confused, especially at pressures less than 15 bar, see the figures (12, 13), which belong to the Gaussian and Lorentzian widths in the two branches, where their charging is not consistent with theoretical studies, and it seems that the dominance is due to the O_2 monomer in the samples, in agreement with reference [13], [22]. Comparing equation (11) and the result from Figure 14, one could calculate the rotational constants from experimental equation (14):

$$\bar{\upsilon} = 13121.407 + 3.1656\,m + 0.00687\,m^2$$
$$m = 0, \pm1, \pm2, \ldots etc \qquad (14)$$

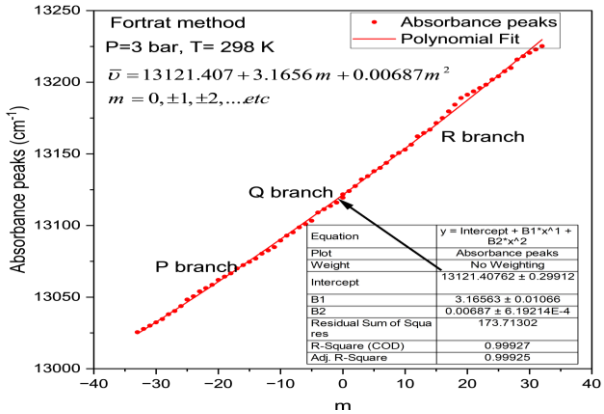

Fig. 14: The Frotrat Method for Absorbance Peaks as A Function m (Quantum Rotational Number (See Equation 7).

From semi-empirical expressions (11), a good value of the rotational constant was deduced:

$$\bar{\upsilon} = \bar{\upsilon}_0 + (B_v' + B_v)m + (B_v' - B_v)m^2 = 13121.407 + 3.1656m + 0.00687m^2$$
$$B_v' + B_v = 3.1656 = d = \Delta\bar{\upsilon}, B_v' - B_v = 0.00687 = e = \frac{1}{2}\Delta^2\bar{\upsilon}$$
$$2B_v' = 3.17247\,cm^{-1}$$
$$2B_v = 3.15873\,cm^{-1}$$
$$B_v' \approx B_v \Rightarrow B \approx 1.5828\,cm^{-1} \qquad (15)$$
$$if\ e \approx 0 \Rightarrow d = 2B_v \Rightarrow \bar{\upsilon} = \bar{\upsilon}_0 + 2B_v m = c + dm$$
$$\bar{\upsilon} = 13121.407 + 3.1656\,m$$
$$m = 0, \pm1, \pm2, \ldots etc$$

From previous calculations, Table 1 shows a summary of the values of $2B_v$ analytically, experimentally, arithmetically, and theoretically.

Table 1: Presents the Results Analytically and Computationally, Compared to the Theoretical Values

Symbol	Slope=d=2Bv	2Bv calc.	2Bv=1st av.=d
Value	3.1656 cm-1	2.86619 cm-1	3.0142 cm-1
$B_v' \approx B_v \Rightarrow B \approx from 1.4 to 1.5828\ cm^{-1}, B_v theoretically\ = 1.4376\ cm^{-1}$			

Figure 15 shows the peaks of maximum absorbance where P and R branches appear clearly with their rotational quantum number, especially the value of J_{max} at which maximum absorbance occurs.
From semi-empirical expressions (8), J maximum could be calculated at the temperatures used in this paper:

$$J_{\max} = \sqrt{\frac{kT}{2Bhc}} - \frac{1}{2} \tag{16}$$

$$(J_{\max})_{298K} = 8.64, \quad (J_{\max})_{323K} = 8.99$$

$$(J_{\max})_{348K} = 9.33, \quad (J_{\max})_{373K} = 9.67$$

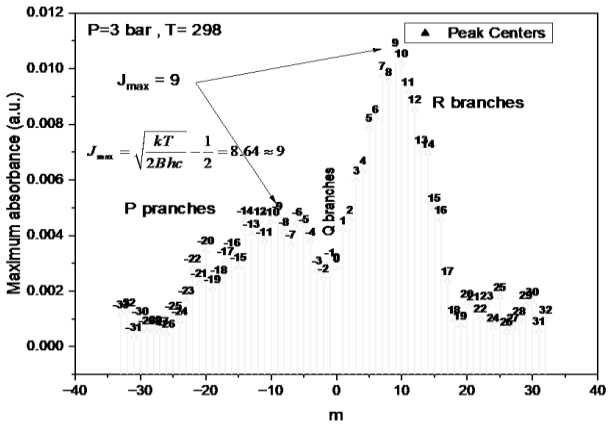

Fig. 15: The Peaks of Maximum Absorbance as A Function of m.

6. Conclusion

This study reinforces the atmospheric and remote sensing research referenced in the introduction. It confirms that in the upper layers of the atmosphere, where atmospheric pressure is low, the concentration of O2 dimol is very low. As a result, it does not significantly contribute to the absorption spectrum in the Oxygen A-band at 762 nm, where the O2 monomer absorption spectrum will prevail.
Because two types of oxygen have the same excitation energy, the absorption spectrum is distorted rather than linear. This distortion results from the interference between the excitation of O_2 dimol and monomeric oxygen.
Temperature changes within the range of 100°C do not seem to cause significant changes in the drop in absorption intensity or the integrated absorbance. Instead, as temperature increases, one would expect the absorption intensity to decrease sharply and the integrated absorbance to become flatter.
The intensity of absorption and the integrated absorption at the peaks of the P and R rotational branches increase linearly with rising pressure, suggesting that the absorption centers remain unchanged despite temperature variations.
The absorption is mainly due to free oxygen molecules, O_2 monomer. Collision-induced absorption (CIA), in the presence of oxygen molecules O_2-O_2 themselves (O_2 dimol), occurs only in the pressure range above 15 bars, and its contribution to the total absorption is small and within the experimental measurement error.
Below 15 bar, Doppler broadening dominates, decreasing with increasing pressure, while pressure broadening increases very slowly over the range of pressures and temperatures considered, which means that the conflict between Doppler and pressure broadening is semi-neglected under 15 bar.

Acknowledgment

I am greatly indebted to Yahia M. Mahzia for his comments and fruitful discussions about this work by private communication, where we have joint research projects in many papers.

References

[1] E. M. Adkins, S. N. Yurchenko, W. Somogyi, J. T. Hodges, "An accurate determination of O2 A-band line intensities through experiment and theory", Journal of Quantitative Spectroscopy and Radiative Transfer 338(2025)109412,ISSN 0022-4073, https://doi.org/10.1016/j.jqsrt.2025.109412.
[2] M. Zhao, H. Zhou, Y. Jiang et al. "Space-Based Limb-Imaging Spectrometer for Atmospheric O_2 Airglow Detection". Atmosphere 16(2025) 214. https://doi.org/10.3390/atmos16020214.
[3] Ze Han, Y. Gong, S. Pang, J. Sun, F. Wang, "Confocal dual-excitation PAS oxygen sensor utilizing 760 nm LED and reshaped differential resonator", Infrared Physics & Technology 145(2025)105707, ISSN 1350-4495, https://doi.org/10.1016/j.infrared.2024.105707.
[4] L. E. Stevenson, J. L. Laughner, M. Okumura, J. T. Hodges, E. M. Adkins, "Contributions of argon, nitrogen, and oxygen to air broadening in the oxygen A-band", Journal of Quantitative Spectroscopy and Radiative Transfer, 342(2025)109480, ISSN 0022-4073, https://doi.org/10.1016/j.jqsrt.2025.109480.
[5] D.A. Long, D.K. Havey, M. Okumura, C.E. Miller, J.T. Hodges, "O2 A-band line parameters to support atmospheric remote sensing", Journal of Quantitative Spectroscopy and Radiative Transfer,111(14) (2010)2021-2036, ISSN 0022-4073, https://doi.org/10.1016/j.jqsrt.2010.05.011.

[6] C. R. Nowlan, C. T. McElroy, J. R. Drummond, J. Quant, "Measurements of the O_2 A- and B-bands for determining temperature and pressure profiles from ACE–MAESTRO: Forward model and retrieval algorithm". Journal of Quantitative Spectroscopy and Radiative Transfer 108(3) (2007)371–388, https://doi.org/10.1016/j.jqsrt.2007.06.006.

[7] Q. Min, L.C. Harrison, E. E. Clothiaux, "Joint statistics of photon path length and cloud optical depth case studies", J Geophys. Res. Atmos 106 (2001)7375–7385, https://doi.org/10.1029/2000JD900490.

[8] D.M. O'Brien, R.M. Mitchell, S.A. English, G.A. Da Costa, "Airborne measurements of air mass from O_2 A-band absorption spectra", J. Atmos. Ocean. Technol. 15 (1998)1272–1286, https://doi.org/10.1175/1520-0426(1998)015<1272:AMOAMF>2.0.CO;2.

[9] A. Kuze, K.V. Chance, "Analysis of cloud-top height and cloud coverage from satellites using the O_2 A-band and B-bands", Journal of Geophysical Research. 99(D7) (1994)14481–14491, https://doi.org/10.1029/94JD01152.

[10] D. M. O'Brien, R.M. Mitchell, "Error-estimates for retrieval of cloud-top pressure using absorption in the A-band of oxygen", Journal of Applied Meteorology, 31(1992) 1179–1192, https://doi.org/10.1175/1520-0450(1992)031<1179:EEFROC>2.0.CO;2.

[11] P. H. Krupenie, "The spectrum of molecular oxygen", J. Phys. Chem. Ref. Data 1(1972) 423-534. https://doi.org/10.1063/1.3253101.

[12] A. Meckler, "Electronic Energy Levels of Molecular Oxygen ", J. Chem. Phys. 21(1953) 1750-1762. https://doi.org/10.1063/1.1698657.

[13] G. D. Greenblatt, John J. Orlando, James B. Burkholder, and A. R. Ravishankara. "Absorption Measurements of Oxygen between 330 and 1140 nm." J. Geophysical Research 95 (D11) (1990)18577-18582. https://doi.org/10.1029/JD095iD11p18577.

[14] A. P. Trushina, V. G. Goldort, S. A. Kochubei, A. V. Baklanov, "UV-photoexcitation of encounter complexes of oxygen O2–O2 as a source of singlet oxygen O2(1Dg) in gas phase", Chem. Phys. Lett. 485 (2010) 11–15. https://doi.org/10.1016/j.cplett.2009.11.058.

[15] C. B. Farmer, J. T. Houghton, "Collision-induced Absorption in the Earth's Atmosphere", Nature 209(1966) 1341 – 1342. https://doi.org/10.1038/2091341a0.

[16] F. R. Spiering, M. B. Kiseleva, N. N. Filippov, Bas van Lieshout, A. van der Veen, and W. J. van der Zande, "The Effect of Collisions with Nitrogen on Absorption by Oxygen in the A-Band Using Cavity Ring-down Spectroscopy." Molecular Physics 109 (4) (2011)535–542. https://doi.org/10.1080/00268976.2010.533709.

[17] H. B. Levine and G. Birnbaum, "Classical Theory of Collision-Induced Absorption in Rare-Gas Mixtures", Phys. Rev. 154(1967)86 –92. https://doi.org/10.1103/PhysRev.154.86.

[18] L. R. Brown, C. Plymate, "Experimental line parameters of the oxygen a band at 760 nm." J. Molec. Spectrosc. 199 (2000)166–179. https://doi.org/10.1006/jmsp.1999.8012.

[19] D. J. Robichaud, Y. Laurence, D. Long, M. Okumura, D. K. Havey, J. T. Hodges, C. E. Miller, and L. R. Brown. "Experimental line parameters of the $b^1\sum_g^+ \leftarrow X^3\sum_g^-$ band of oxygen isotopologues at 760 nm using frequency-stabilized cavity ring-down spectroscopy." J. Phys. Chem. A 113 (47) (2009)13089–13099. https://doi.org/10.1021/jp901127h.

[20] D. J. Robichaud, J. T. Hodges, P. Masłowski, L. Y. Yeung, M. Okumura, C. E. Miller, and L. R. Brown. "High-accuracy transition frequencies for the O_2 a-band." J. Molec. Spectrosc. 251 (1-2) (2008)27–37. https://doi.org/10.1016/j.jms.2007.12.008.

[21] S. Wójtewicz, A. Cygan, P. Masłowski, J. Domysławska, D. Lisak, R.S. Trawiński, R. Ciuryło. "Spectral Line Shapes of Self-Broadened P-Branch Transitions of Oxygen B Band." J. Quantitative Spectroscopy and Radiative Transfer 144(2014) 36–48. https://doi.org/10.1016/j.jqsrt.2014.03.029.

[22] H. Tran, C. Boulet, J.-M. Hartmann. "Line-mixing and collision-induced absorption by oxygen in the a-band. Laboratory measurements, model, and tools for atmospheric spectra computations" J. Geophysics. Research, 111(2006),1-14, D15210. https://doi.org/10.1029/2005JD006869.

[23] M. V. Tonkov, N. N. Filippov, Yu M. Timofeyev, V. Polyakov. "A simple model of the line mixing effect for atmospheric applications: theoretical background and comparison with experimental profiles." Journal of Quantitative Spectroscopy and Radiative Transfer 56 (5) (1996)783–795. https://doi.org/10.1016/S0022-4073(96)00113-6.

[24] M. Vangvichith, H. Tran, J. M. Hartmann. "Line-mixing and collision-induced absorption for O_2-CO_2 mixtures in the oxygen a-band region." Journal of Quantitative Spectroscopy and Radiative Transfer 110 (18) (2009) 2212–2216. https://doi.org/10.1016/j.jqsrt.2009.06.002.

[25] F. R. Spiering, M. B. Kiseleva, and N. N. Filippov, et al. "Line mixing and collision-induced absorption in the oxygen a-band using cavity ring-down spectroscopy." J. Chem. Phys. 133, (2010)114305-114309. https://doi.org/10.1063/1.3460924.

[26] J.-M. Hartmann, H. Tran, and G. C. Toon. "Influence of line mixing on the retrievals of atmospheric co$_2$ from spectra in the 1.6 and 2.1 μm regions." Atmospheric Chemistry and Physics Discussions 9 (1) (2009)4873–4898. https://doi.org/10.5194/acpd-9-4873-2009.

[27] M. Born and J. R. Oppenheimer, "On the quantum theory of molecules", Ann. Physik-Leipzig, 84(1927) 457-484. https://doi.org/10.1002/andp.19273892002.

[28] H.H. Nielsen, "The vibration-rotation energies of molecules and their spectra in the infra-red". Encyclopedia of Physics / Handbuch der Physik, 7 (1959)37 / 1. Springer, Berlin, Heidelberg. https://doi.org/10.1007/978-3-642-45917-7_2.

[29] J. M. Brown and A. Carrington, "Rotational spectroscopy of diatomic molecules", Cambridge University Press, New York, 2003. https://doi.org/10.1017/CBO9780511814808.

[30] G. Herzberg, "Molecular spectra and molecular structure I. Spectra of diatomic molecules", 2nd edition, Van Nostrand Reinhold, New York. (1950).

[31] J. Domysławska, S. W´ojtewicz, A. Cygan, et al. "Low-pressure line-shape study in molecular oxygen with absolute frequency reference". J. Chem. Phys. 139(2013)194312-194322. https://doi.org/10.1063/1.4830219.

[32] J. Domysławska, S.W´ojtewicz, P. Masłowski, et al." Spectral line shapes and frequencies of molecular oxygen B-band R-branch transitions". J. Quant. Spectrosc. Radiat. Trans. 155(2015)22-31. https://doi.org/10.1016/j.jqsrt.2014.12.015.

[33] H.H. Deslandres, "The Vibration-rotation Energies of Molecules and their Spectra in the Infra-red" C. R. Paris 103(1886)375

[34] M. A. AL-Jalali, I. F. Aljghami, and Y. M. Mahzia, "Absorption Spectrum Deconvolution of Zero Air at 1270 nm Band", Int. J. ChemTech Res. 8(2015)116-127. CODEN (USA): IJCRGG. ISSN: 0974-4290.

[35] M. A. AL-Jalali, Y. M. Mahzia, "Competition between Lorentzian Gaussian width in pure oxygen absorption spectrum at 1264 nm band", 46(2017)241–246. https://doi.org/10.1007/s12596-017-0409-y.

[36] M. A. AL-Jalali, I. F. Aljghami, and Y. M. Mahzia, "Voigt deconvolution method and its applications to pure oxygen absorption spectrum at 1270 nm band", Spectrochim. Acta Part A Mol. Spectrosc. 157(2016)34-40. https://doi.org/10.1016/j.saa.2015.12.010.

[37] M. A. AL-Jalali, "Comparison between simple and advanced data analysis to pure oxygen absorption spectrum at the 1270 nm band", J. Appl. Math. Phys. (JAMP) 3(2015)1114–1121. https://doi.org/10.4236/jamp.2015.39138.

[38] Y. Liu, J. Lin, G. Huang, Y. Guo, and C. Duan," Simple empirical analytical approximation to the Voigt profile", Journal of the Optical Society of America B, 18,(2001)666-672 https://doi.org/10.1364/JOSAB.18.000666.

[39] F.G. Lether, P.R. Wenston, "The numerical computation of the Voigt function by a corrected midpoint quadrature rule for $(-\infty, \infty)$", Journal of Computational and Applied Mathematics,34,1(1991)75–92. https://doi.org/10.1016/0377-0427(91)90149-E.

[40] J. Humlíček, "Optimized computation of the Voigt and complex probability functions", J. Quant. Spectrosc. Radiat. Transfer 27(1982)437- 444. https://doi.org/10.1016/0022-4073(82)90078-4.

[41] G. Pagnini, R.K. Saxena, "A note on the Voigt profile function", J. Phys. A: Math. Gen, 1(2008)1-13.arXiv: 0805.2274v1, https://doi.org/10.48550/arXiv.0805.2274

[42] Y.-R. Xu, A.-W. Liu, Y. Tan, C.-L. Hu, and S.-M. Hu, "Saturated absorption spectroscopy of M1 transitions of O 2 near 764 nm", PHYSICAL REVIEW A 109, (2024) 042809. https://doi.org/10.1103/PhysRevA.109.042809.

[43] H. Tran, J.-M. Hartmann, "An improved O2 A band absorption model and its consequences for retrievals of photon paths and surface pressures", JOURNAL OF GEOPHYSICAL RESEARCH, 113, (2008)D18104. https://doi.org/10.1029/2008JD010011.

[44] S. Fally, C. Hermans, A.C. Vandaele, M. Carleer, L. Daumont, and A. Jenouvrier, 2006. "The Ninth Biennial HITRAN Conference". Poster 2.4.

[45] M. A. AL-Jalali, "Pressure broadening and narrowing due to oxygen and nitrogen gas mixtures at 1270 nm band: part III", International Journal of Physical Research, 12 (2) (2024) 29-35, https://doi.org/10.14419/a2831v85.